Development of Photon Calibrator for Hardware Injection Test

Yu-Kuang Chu

國立臺灣師範大學

Recommended for Acceptance

by the Department of

Physics

Adviser: Wo-Lung Lee Sadakazu Haino

June 2018

Abstract

This is a LaTeX template and document class for Ph.D. dissertations at Princeton University. It was created in 2010 by Jeffrey Dwoskin, and adapted from a template provided by the math department. Their original version is available at: `http://www.math.princeton.edu/graduate/tex/puthesis.html`

This is **NOT** an official document. Please verify the current Mudd Library dissertation requirements [**?**] and any department-specific requirements before using this template or document class.

Your abstract can be any length, but should be a maximum of 350 words for a Dissertation for ProQuest's print indicies (or 150 words for a Master's Thesis); otherwise it will be truncated for those uses [**?**].

Dwoskin Ph.D. Dissertation Template — version 1.0, 5/19/2010

Acknowledgements

I would like to thank the Math department for providing the original documentclass file that this class is based upon. I would like to thank my parents, without whom my life would not be possible. I would also like to thank my advisor, my dissertation committee, and my research collaborators because every graduate student needs to do so. And finally, I thank the members of my research group, to whom I leave this template to save you some of the trouble I had to go through getting my dissertation to compile in LaTeX.

Don't forget to ask your advisor if your work was sponsored by a grant that needs to be acknowledged in this section.

To my parents.

Contents

List of Tables

List of Figures

Chapter 1

Introduction

When you got a new camera, you probably will take a lot of testing photos before you start to use it seriously. Similarly, we would like to test our gravitational wave detector before we use it to see the Universe.

Hardware injection test is a process to verify the performance of interferometer by sending sample signals into interferometer. Ideally, we should prepare some real gravitational waves as test signals. But it is practically hard to generate large enough artificial gravitational waves that are detectable by current technology.

Therefore, instead of generating gravitational waves, people mimic the effect of celestial gravitational waves by displacing the mirror according to the simulated gravitational waveforms, changing arm length correspondingly, , comparing the optical readout in the main interferometer, thereby checking the response of their interferometer.

Among different ways to push those Test Mass Mirrors in the main interferometer, radiation pressure of external laser beams have been used because its simplicity and stability. A dedicated auxiliary laser system called Photon Calibrator(PCal) has been developed for this purpose.

In this dissertation, I will briefly explain what is photon calibrator and how it works for calibration and hardware injection purposes. Then, I will discuss the noise problem from current signal generating system that is used to control PCal Laser intensity. Finally, a possible solution, Analog De-Whitening Filter, has been manufactured and tested with Photon Calibrator in Kamioka Gravitational Wave Detector (KAGRA).

1.1 Introduction to Gravitational Wave

1.1.1 What is gravitational wave

In the General Theory of Relativity proposed by Albert Einstein in 1915, phenomena caused by gravity can be interpreted as results of curved spacetime. This is one of his important works after his ‘Happiest Thought’, which recorded in his unpublished article “Fundamental Ideas and Methods of the Theory of Relativity, Presented in Their Development”[1]. Among different ways to curve our spacetime, which can be described by corresponding metric tensor fields, there exist wavelike solutions describing ripples of spacetime known as gravitational waves.

However, the physical reality of gravitational wave was not so clear to everyone in the early days, even to Einstein himself [2, 3]. The main problem is that there exist some gauge degree of freedom in the theory due to the arbitrariness of coordinate choices. We have to know whether the gravitational waves we found are just gauge waves (vibration of coordinate) or the wave can have some observable consequences.

One of the most important observational evidence implying the existence of real gravitational waves is the Hulse-Taylor pulsar [4]. Taylor demonstrated that the change of pulsar rotation speed can be explained by emission of gravitational wave [5, 6].

Finally, on September 14th, 2015, the first direct detection of gravitational wave signal [7] is done by Laser Interferometer Gravitational-Wave Observatory(LIGO) detectors in the United States.

1.1.2 How to describe gravitational wave

In Einstein's General Relativity, gravitational effects are realized by geometry of spacetime. According to a great mathematician Bernhard Riemann, we can describe the geometry of certain space by telling the "distance" between nearby points in the space. Practically, the information of distance between nearby spacetime points form a tensor called metric, which means the measure of distance. By choosing a coordinate system, one can write down those corresponding components of metric tensor g.

$$g_{\mu\nu} = \begin{pmatrix} g_{00} & g_{01} & g_{02} & g_{03} \\ g_{10} & g_{11} & g_{12} & g_{13} \\ g_{20} & g_{21} & g_{22} & g_{23} \\ g_{30} & g_{31} & g_{32} & g_{33} \end{pmatrix} \tag{1.1}$$

Now, we can calculate spacetime distance ds between two nearby points by their coordinate separation:

$$ds^2 = g_{\mu\nu} dx^\mu dx^\nu \tag{1.2}$$

Through the interaction between matter and spacetime, matter can curve our Universe. The whole story can be resolved by solving Einstein equation,

$$R_{\mu\nu} - \frac{1}{2} g_{\mu\nu} R = \frac{8\pi G}{c^4} T_{\mu\nu} \tag{1.3}$$

which is a non-linear differential equation of metric tensor field $g_{\mu\nu}(x^\alpha)$ since the Ricci tensor $R_{\mu\nu}$ contains metric tensor and its differential.

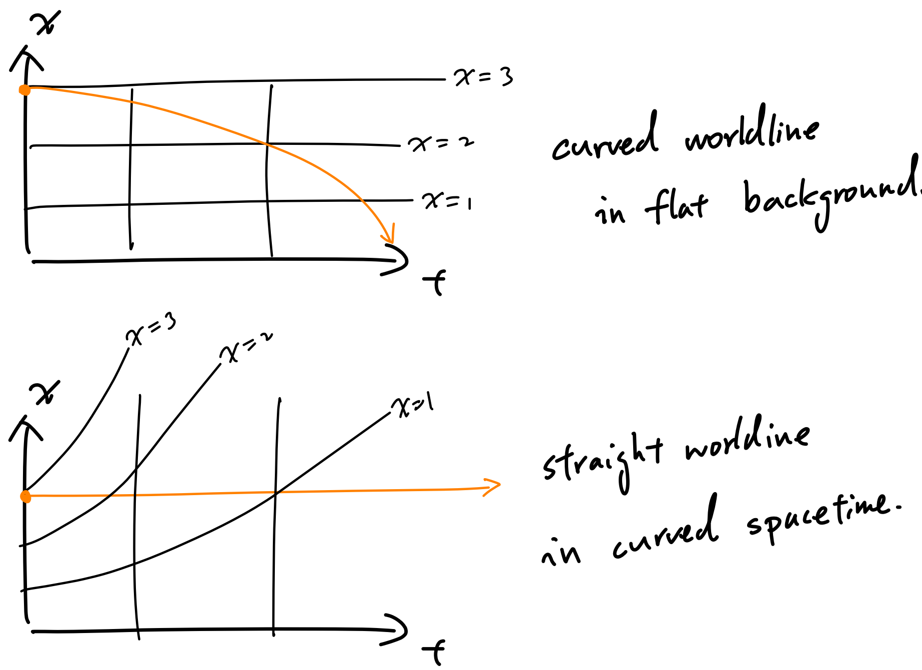

Figure 1.1: Newtonian versus Einstein's point of view.

It's similar to the case in Electrodynamics, in which we can have electromagnetic waves solutions by solving Maxwell equations in vacuum, that we can have gravitation wave solutions by solving vacuum Einstein equation. The situation will become even clear if we linearize the Einstein equation and choose coordinate or gauge properly.

Let's start from

$$\Box \bar{h}_{\mu\nu} = -\frac{16\pi G}{c^4} T_{\mu\nu} \tag{1.4}$$

the corresponding coordinates are attached to a set of free falling objects. for perturbation of wave like part metic over Schwarzschild background which represent Earths gravity.

Refer to [8]

How to generate gravitational wave The source of electromagnetic wave is time-dependent electrical charge distribution. Similarly, the source of gravitational wave is time-dependent mass(energy) distribution. Strictly speaking, the lowest order of mass multi-pole which can generate real gravitational waves is mass quadruple because we dont have negative mass, while the electromagnet wave can be generate though time-dependent electrical dipole moment. The gravitational wave strain generated by mass quadruple can be approximately described by famous quadrupole formula: (quadrupole formula) Practically, PN NR.... According to our current understand of universe, there are several kinds of astrophysical gravitational wave sources, whose h(t) amplitude is large enough to be detected by current ground based laser interferometer, like advanced-LIGO, advanced-Virgo or KAGRA. Compact Binary Coalescence BNS BBH

1.1.3 How to detect Gravitational wave

The interaction of detector and gravitational wave can have different interpretation due to different coordinate choice[9]. It is quiet similar to that the magnetic force in one observational frame may be electric force in the other frame. However, practically, I would like to use the .., which described in next section.

1.2 Detection of Gravitation wave

Interaction of GW wave when $\lambda_g w$ L of detector Limit of Michelson IFO IFO with dual-recycling and Fabry-Perot arms. Complex response WE NEED Calibration Calibration Calibration

1.3 Calibration and Reconstruction

Calibration is always the fist step before we measure something by some device. For example, to measure the weight of an apple, you should calibrate your scale by putting a standard kilogram on it. Then, you can either adjust the scale readout to be 1kg, or record the difference showed in scale readout, which may be used to reconstruct real weight of the apple. However, the spring constant of springs inside the scale could fluctuate due to temperature changes. To accurately measure the weight of the apple, we have to measure the calibration factor (scale readout when we put the standard mass on it.) when we measure the weight of apple, if possible, simultaneously.

Due to the complexity of practical interferometer, the response of interferometer itself to external gravitational source is not only sophisticated but also time-dependent. In reality, we inject several calibration lines, which means we displace the End-Test-Mirror by several known frequency and amplitude sine waves. Then, we try to see these standard signals in the readout of interferometer, thereby solving the response of interferometer.

1.3.1 Transfer function of Laser Interferometer with Fabry-Perot Cavity

1.3.2 Tracking Time-dependent Response by Calibration lines

1.4 Photon Calibrator (Pcal)

1.4.1 Principle of Photon Calibrator

Photon calibrator is an additional laser with high precision intensity modulator. It is installed in front of End-Test-Mass Mirror(ETM) and can push the ETM by radiation force due to its own Laser beam as depicted in Fig.(XX). To generate any artificial h(t) by Pcal, we have to translate desired h(t) into corresponding force F(t) exerting on ETM. This can be done by using equation of motion of the ETM suspend by its suspension system. Then, we control the Pcal Laser output intensity P(t) such that the radiation force exerted on ETM is F(t) we calculated before.

The radiation force caused by a continuous laser beam can be calculated by its momentum transfer per unit time.

$$\mathbf{F} = \frac{\Delta \mathbf{p}}{\Delta t} \tag{1.5}$$

For our purpose, the laser beam will be almost reflected from ETM. Therefore, the momentum transfer to ETM per unit time should be almost equal to twice of longitudinal momentum flux carried by PCal laser beam.

$$\mathbf{F}_{\text{on ETM}} = \frac{\Delta \mathbf{p}_{\text{ETM}}}{\Delta t} = 2\cos(\theta)\frac{\Delta p_{\text{Laser}}}{\Delta t} \tag{1.6}$$

where θ is the angle of incident.

Furthermore, one can express the momentum flux of light in terms of its intensity through Eq.(1.10), which can be derived from either classical point of view with its Poynting vector or Quantum Mechanical approaches that we adopt here by dealing with photons.

$$E_\gamma = \hbar\omega \tag{1.7}$$

$$p_\gamma = \hbar k \tag{1.8}$$

$$= \frac{k}{\omega}\, E_\gamma = \frac{1}{c} E_\gamma \tag{1.9}$$

$$\underbrace{\frac{\Delta p_{\text{photons}}}{\Delta t}}_{\substack{\text{momentum flux due to} \\ \text{photons in a continuous laser beam}}} = \frac{1}{c}\; \underbrace{\frac{\Delta E_{\text{photons}}}{\Delta t}}_{\substack{\text{Intensity of laser beam} \\ \text{defined as } P}} = \frac{P}{c} \tag{1.10}$$

Combining Eq.(1.6) and Eq.(1.10), the force that PCcal can give ETM is:

$$F_{\text{PCal}}(t) = \frac{2\cos(\theta)}{c} P(t) \tag{1.11}$$

On the other hand, the equation of motion of suspend ETM can be modeled as:

$$\ddot{x}(t) + b\dot{x}(t) + \omega_0^2 x(t) = \frac{F(t)}{M} \tag{1.12}$$

The impulse response is

$$x(t) = \frac{b}{\omega_1} e^{-\frac{b}{2}(t-t_0)} \sin[\omega_1(t-t_0)] \tag{1.13}$$

And the transfer function is

$$x(\omega) = \frac{-1}{\omega^2 - \omega_0^2 + i\omega b} F(\omega) \tag{1.14}$$

As long as $\omega^2 \gg \omega_0^2$ and $\omega \gg b$, Eq.(1.14) can be approximated as

$$x(\omega) = \frac{-1}{\omega^2} F(\omega) \tag{1.15}$$

By substituting the Fourier transformed Eq.(1.11) into it, we can get the expression of x(f) introduced by P(f)

$$x(\omega) = \frac{-1}{M\omega} \frac{2P(f)\cos(\theta)}{c} \tag{1.16}$$

1.4.2 Evolution of Photon Calibrator

Original Pcal is proposed by Glasgow group [10]. They use single laser beam hitting on the center of ETM and successfully see these sin waves in the the readout of their interferometer. Later on, GEO...

is that it may introduce drumhead mode vibration of ETM surface (just like the vibration mode you see when you hit the center of a drum), which introduce unwanted h(t) effectively. This problem is solved by LIGO group[11], who separate the Pcal laser beam into two beams, hitting on the nodal point of drumhead mode on the ETM surface[12].

In order to excite same amplitude h(t) in higher frequency regime, we have to give much larger F(t) since the relationship between x(t) and F(t) in an pendulum .

1.4.3 Why do we need Photon Calibrator

1.4.4 Tracking Time-dependent Response by Calibration lines

Chapter 2

Hardware Injection through Photon Calibrator

2.1 Principle

Amplitude of Injection Signal

$$\frac{F(t)}{M} = \frac{1}{M}\frac{2P(t)\cos(\theta)}{c} = \ddot{x}(t) \tag{2.1}$$

For $x = x_0 \sin(\omega t)$,

$$\frac{1}{M}\frac{2P_0\cos(\theta)}{c}\sin(\omega t) = -\omega^2 x_0 \sin(\omega t) \tag{2.2}$$

Thus,

$$P_0 = -\omega^2 \frac{Mc}{2\cos(\theta)} x_0 = -\omega^2 \frac{Mc}{2\cos(\theta)} L h_0 \tag{2.3}$$

$$M = 23 \text{ kg}$$

$$L = 3 \text{ km}$$

$$\theta = 0.72 \text{ deg}$$

$$c = 2.998 \times 10^8 \text{ m/s}$$

$$P_0 \text{ (Watts)} \times \frac{Gain_{\text{ Power to OFSPD}}}{2} = \underbrace{V_{\text{OFSPD}}}_{\text{Same as V}_{\text{Injection}}} \quad \text{(Volts)}$$

Therefore, the overall gain should be set in injection channel, which is in Volt unit, is

$$\omega^2 \frac{Mc}{2\cos(\theta)} L \times \frac{Gain_{\text{ Power to OFSPD}}}{2} \tag{2.4}$$

Chapter 3

Signal Generating System

3.1 KAGRA Digital System as Signal Generator

The Digital Control System used in KAGRA is based on the Advanced LIGO Digital System. In this system, analog control signals can be generated from a Digital-Analog Convertor(DAC) installed in any realtime computer known as a Front-End machine in the tunnel. Between the DAC output and experimental device, a customized analog low-pass filter called an Anti-Image filter has been installed for removing unwanted high frequency signal, the Image, due to digitized output from DAC.

Inside the Front-End machines, the signal that will be sent to DAC are prepared by realtime software, which is generated from several building blocks, the realtime models, by customized parser and compiler. Each realtime model will be running at specifiable sample rate on a dedicated CPU core. However, currently, all DAC cards installed at KAGRA site are 16bit, 64kHz (65536Hz) ones. Therefore, a mandatary model named Input/Output Processor(IOP) model will always run at 64kHz, communicating with a DAC card and other "slave" models, in which

(people)

can put digital filters, signal generators, etc.

3.2 Noise Problem of Injection Signal

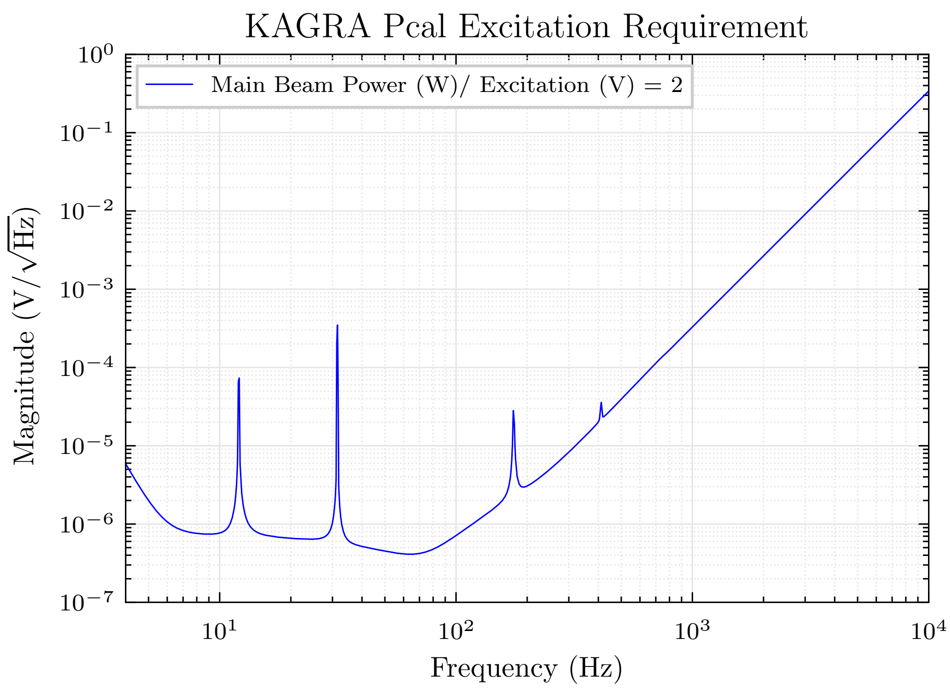

Figure 3.1: Injection Channel Noise Requirement

$$\Delta L(f) < \frac{1}{10} \times (\text{KAGRA length sensitivity}) \tag{3.1}$$

$$\Delta L(f) = \frac{2\Delta P(f)\cos(\theta)}{c}\frac{1}{M(2\pi f)^2} < \frac{1}{10}\Delta h(f)L \tag{3.2}$$

3.2.1 Noise Sources from Control Signal

Quantization Noise of DAC

The origin of quantization error is coming from the difference between desired analog output and quantized Digital to Analog Converter(DAC) output value. Roughly speaking, it shows up like white noise that is spread from DC to Nyquist frequency, i.e. $Fs/2$. The Root Mean Square value of quantization noise has the order of voltage difference corresponding to last digit or Least Significant Bit(LSB). In time domain, we can calculate standard deviation.

$$\sigma_x = \sqrt{\frac{1}{12}}\delta x_{LSB} \tag{3.3}$$

For a 16-bit 64kHz DAC with output range between ±10Volts,

$$\begin{aligned} \sigma_x &= \sqrt{\frac{1}{12}}\delta x_{LSB} && (3.4)\\ &= \sqrt{\frac{1}{12}}\frac{(+10)-(-10)\text{Volts}}{2^{16}} && (3.5)\\ &= 8.81\times 10^{-5}\text{ Volts} && (3.6) \end{aligned}$$

In frequency Domain, the quantization noise is distributed from DC to 32768Hz; therefore, we have ASD

$$\begin{aligned} ASD &= \sqrt{PSD} && (3.7)\\ &= \sqrt{\frac{\sigma_x^2}{32768}} && (3.8)\\ &= 8.81\times 10^{-5}\sqrt{\frac{1}{32768}} && (3.9)\\ &= 4.87\times 10^{-7}\text{ Volts}/\sqrt{\text{Hz}} && (3.10) \end{aligned}$$

Analog circuits

AC Power Line

Chapter 4

Noise Reduction through De-Whitening Filter

4.1 Concept of De-Whitening Filter

Considering a situation in which the Photon Calibrator received white, i.e. frequency independent, excitation signal noise, it will generate $1/f^2$ displacement noise on End-Test-Mirror because the force to displacement transfer function contains $1/f^2$ feature. If we put an analog filter that has frequency response proportional to f^2 between excitation signal and PCal excitation input port, we may create colored, f^2, laser intensity noise from white electrical noise of excitation signal. Then, such colored noise will be whitened by $1/f^2$ force to displacement transfer function, becoming white displacement noise. We call the f^2 analog filter *De-Whitening filter*.

Practically, we use a one pole one zero analog filter with transfer function described in (ref) as our De-Whitening filter.

4.2 Circuit Design

The main circuit design is described in Fig. 4.1. The pole and zero frequency is determined by resistors and capacitors between A and B. We use 0.01μF Mica capacitor(CD30FD103FO3F made by Cornell Dubilier Electronics), whose capacitance tolerance is within 1% and capacitance drift is within $\pm(0.05\% + 0.1pF)$ to reduce filter shape uncertainty caused by pole-zero frequency drifting.

The Transfer function of this circuit is

$$\text{DewTF} = \underbrace{\frac{Z_A}{Z_A + Z_B}}_{\text{pole-zero stage}} \times \underbrace{2}_{\text{Single to Differential}} \tag{4.1}$$

where

$$A//B \equiv \frac{1}{\frac{1}{A} + \frac{1}{B}} \tag{4.2}$$

$$Z_B = (R_3 + \frac{1}{i\omega C_2}) \ // \ R_b \tag{4.3}$$

$$Z_A = (R_4 + \frac{1}{i\omega C_1}) \ // \ R_a \tag{4.4}$$

When $R_3 = R_4 = a$, $C1 = C2 = C$, Eq. (4.1) will reduce to

$$\text{DewTF} = 2\left(\frac{1 + i\omega C(a + R_b)}{1 + \frac{R_b}{R_a} + i\omega C(2R_b + a(1 + \frac{R_b}{R_a}))}\right) \tag{4.5}$$

Practically, we will choose $a = 100\Omega << R_a = 8.34(88)\text{k}\Omega < R_b = 159.(3)\text{k}\Omega$. For DC, the gain is

$$\text{DewTF}\ |_{\omega=0} = \frac{2}{1 + \frac{R_b}{R_a}} = 0.0996 \tag{4.6}$$

It's about factor of ten suppression while the signal gain in high frequency keeps unity. The pole and zero frequencies of such circuit are

$$\text{Zero} = \frac{1}{2\pi C(a + R_a)} = OOO\text{Hz} \tag{4.7}$$

$$\text{Pole} = \frac{1}{2\pi C(a + 2\frac{R_a R_b}{R_a + R_b})} = OOO\text{Hz} \tag{4.8}$$

A simulated overall transfer function by LTspice is showed in Fig. XX

4.3 Fidelity of Injection Signal

The fidelity of injected signal is the fundamental requirement of hardware injection test. One can estimate the distortion of injected waveforms by measuring transfer function between excitation port in the software and PCal laser intensity. With De-Whitening filter, although we

4.4 Noise Reduction Performance

In principle, a

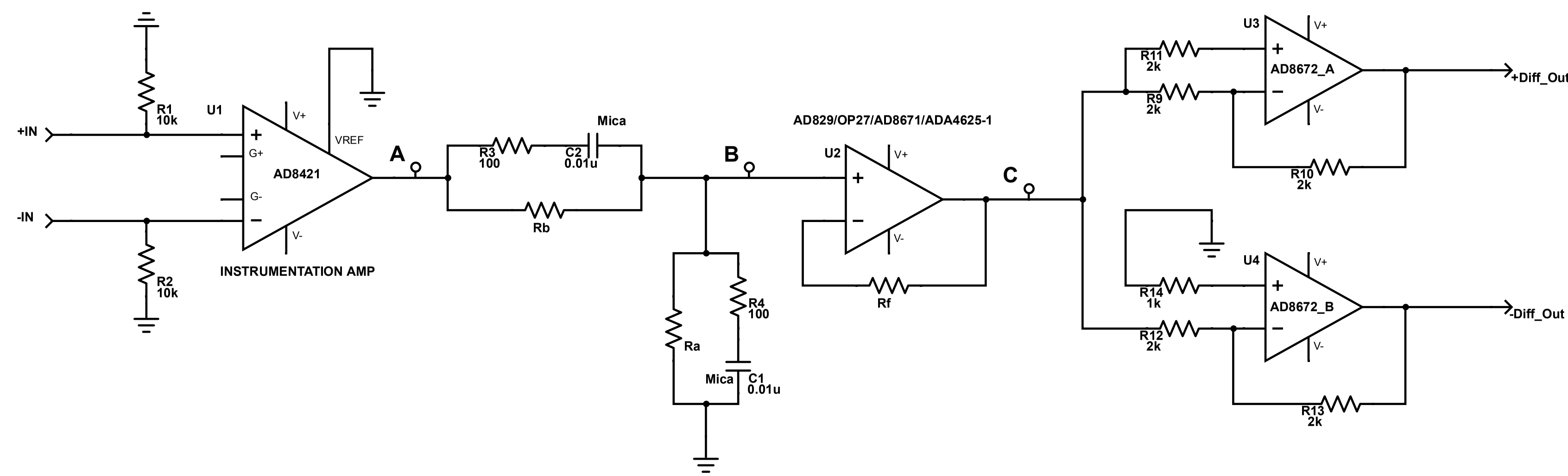

Figure 4.1: De-Whitening filter circuit. There are three points labeled as A, B,and C in the diagram. Before A, the differential input signal provided by Digital System will be converted into single single by a instrumentation amplifier AD8421. After that, a passive pole zero stage between A and B defines the dominate transfer function of De-Whitening filter. Then we put a voltage follower between B and C as a buffer to keep passive filter response. Finally, we convert signal back to differential signal to match downstream device input.

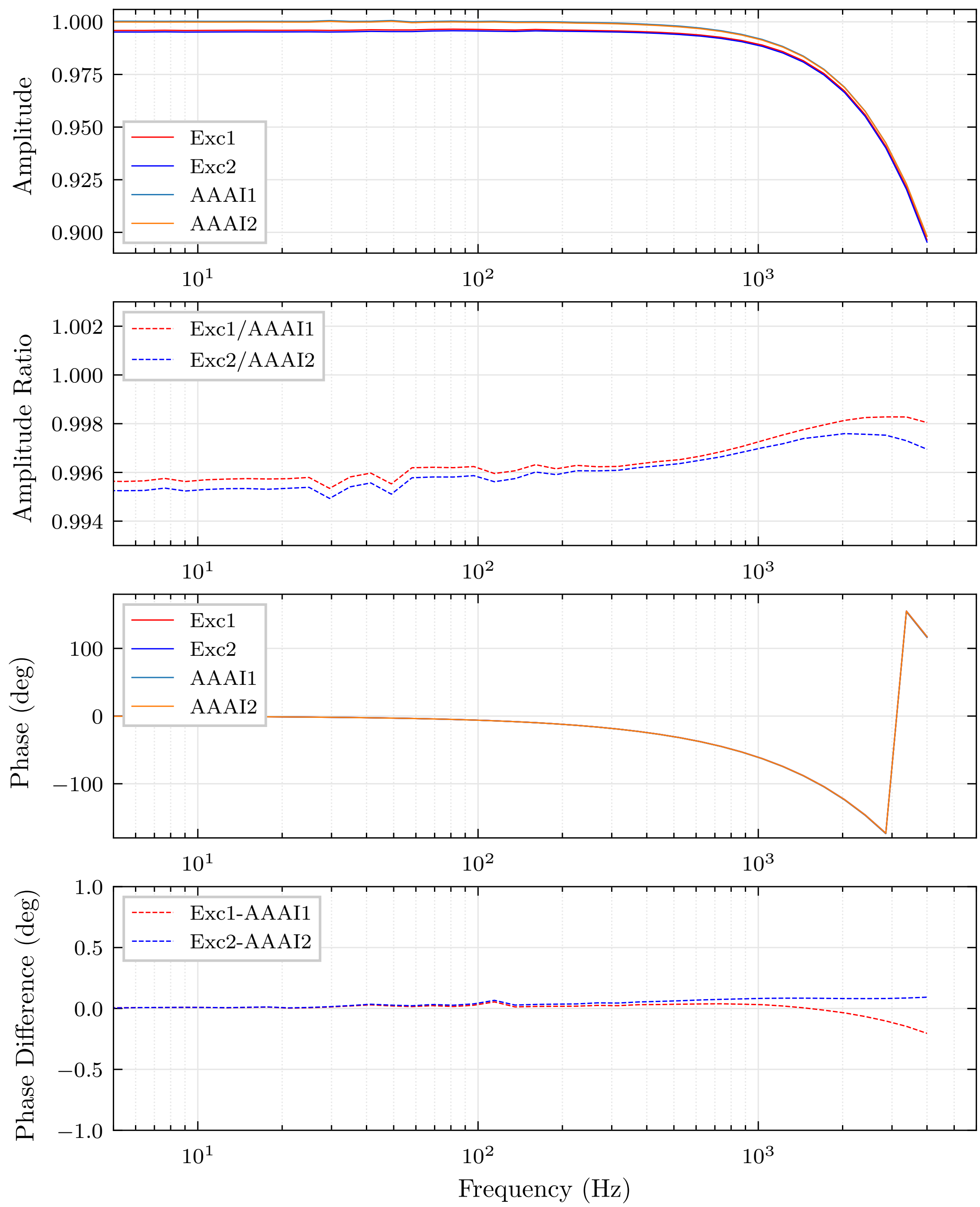

Figure 4.2: Transfer function of De-Whitening Filter with Digital Inverse Filter. The transfer function is measured in KEK cryogenic center with KAGRA standalone digital system and 64kHz salve model.

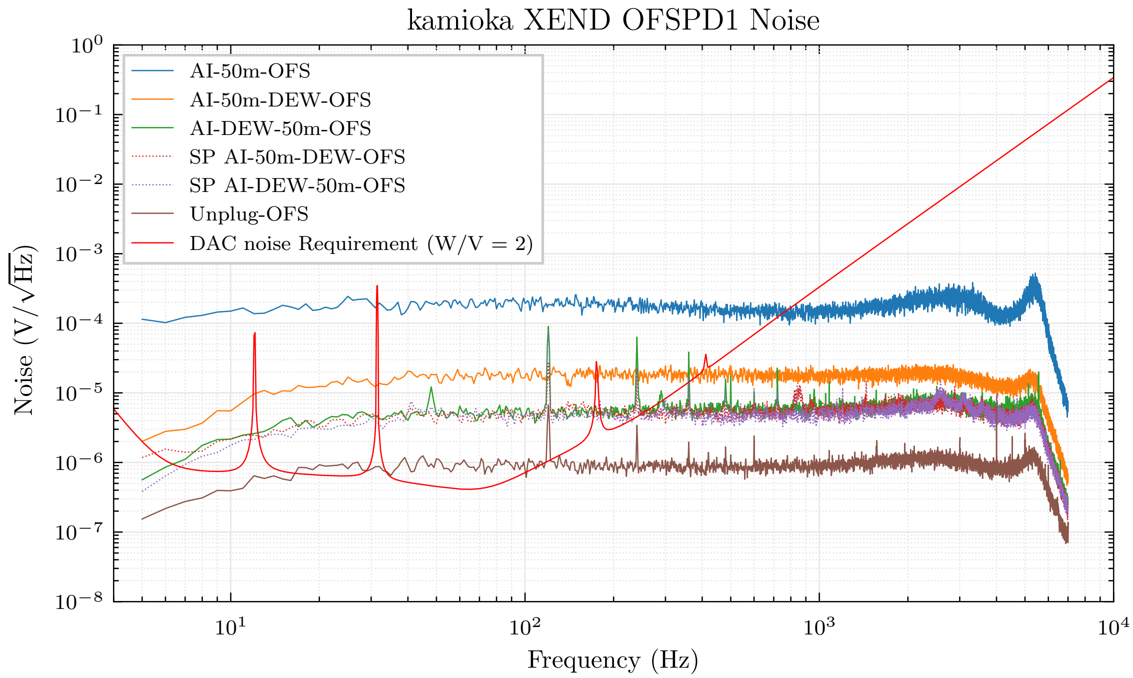

Figure 4.3: Noise

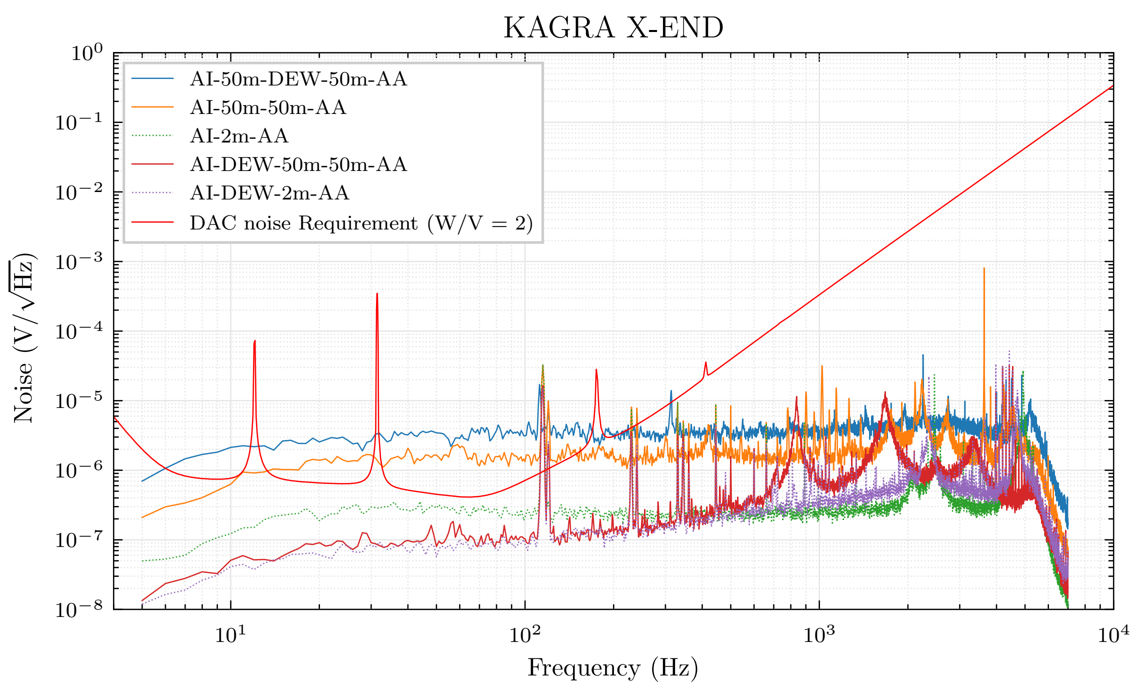

Figure 4.4: Noise

Chapter 5

Validation of Injection Channel

Without loss of generality, We injected binary blackhole signals to test performance of our De-Whitening Filter. Unfortunately we couldn't find a compatible data-taking system with desired noise level and dynamical range to reconstruct or estimate the expect End-Test Mirror (ETM) that generated by our Photon Calibrator.

Besides, We have tried to inject Sine-Gaussian signals.

Noise measurement around 100Hz the nose should below the IFO sensitivity Transfer Function measurement above 1kHz performance time delay of excitation channel (absolute timing measurement?) Distortion of Scientific Signal BBH BNS post merger

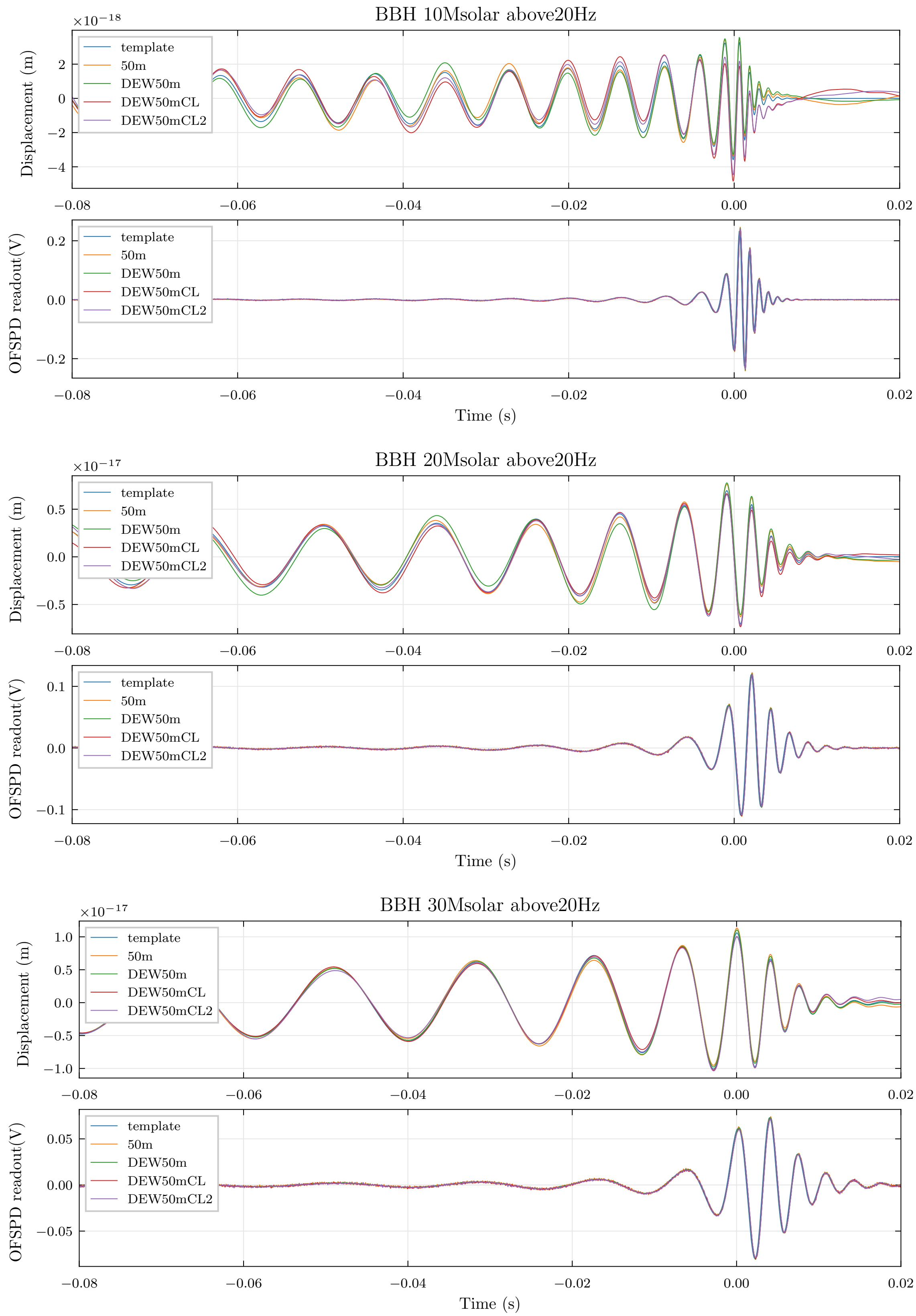

Figure 5.1: Injected Binary Blackhole Merger Signal

Chapter 6

Discussion and Future Works

Ideally, although the De-Whitening Filter can effectively increase low frequency signal resolution, it limits the maximum excitation signal can be sent to Photon Calibrator. In Fig.6.1 we estimated how much dynamical range will be sacrificed.

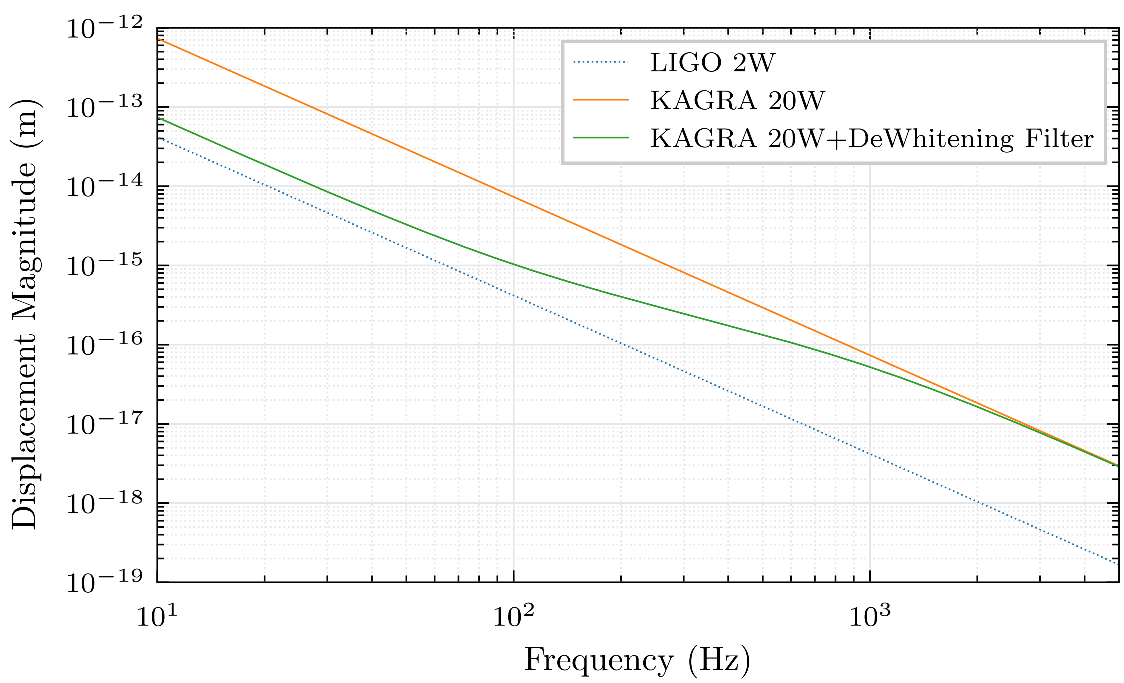

Figure 6.1: Maximum Injection Capability

Bibliography

[1] A Einstein. Grundgedanken und Methoden der Relativitätstheorie, in ihrer Entwicklung dargestellt. Fundamental Ideas and Methods of the Theory of Relativity, Presented in Their Development, after 22 Jan 1920. 1920. URL `https://einsteinpapers.press.princeton.edu/vol7-trans/129`.

[2] Daniel Kennefick. Einstein versus the physical review. *Physics Today*, 58(9):43–48, 2005. doi: 10.1063/1.2117822. URL `https://doi.org/10.1063/1.2117822`.

[3] A. Einstein and N. Rosen. On gravitational waves. *Journal of the Franklin Institute*, 223(1):43 – 54, 1937. ISSN 0016-0032. doi: https://doi.org/10.1016/S0016-0032(37)90583-0. URL `http://www.sciencedirect.com/science/article/pii/S0016003237905830`.

[4] R. A. Hulse and J. H. Taylor. Discovery of a pulsar in a binary system. *ApJ*, 195:L51–L53, January 1975. doi: 10.1086/181708.

[5] J. H. Taylor and J. M. Weisberg. A new test of general relativity - Gravitational radiation and the binary pulsar PSR 1913+16. ApJ, 253:908–920, February 1982. doi: 10.1086/159690.

[6] Joseph H. Taylor. Binary pulsars and relativistic gravity. *Rev. Mod. Phys.*, 66: 711–719, Jul 1994. doi: 10.1103/RevModPhys.66.711. URL `https://link.aps.org/doi/10.1103/RevModPhys.66.711`.

[7] B. P. Abbott et al. Observation of gravitational waves from a binary black hole merger. *Phys. Rev. Lett.*, 116:061102, Feb 2016. doi: 10.1103/PhysRevLett.116.061102. URL `https://link.aps.org/doi/10.1103/PhysRevLett.116.061102`.

[8] M. Maggiore and Oxford University Press. *Gravitational Waves: Volume 1: Theory and Experiments*. Gravitational Waves. OUP Oxford, 2008. ISBN 9780198570745. URL `https://books.google.com.tw/books?id=AqVpQgAACAAJ`.

[9] Malik Rakhmanov. Response of test masses to gravitational waves in the local lorentz gauge. *Phys. Rev. D*, 71:084003, Apr 2005. doi: 10.1103/PhysRevD.71.084003. URL `https://link.aps.org/doi/10.1103/PhysRevD.71.084003`.

[10] DA Clubley, GP Newton, KD Skeldon, and J Hough. Calibration of the glasgow 10 m prototype laser interferometric gravitational wave detector using photon pressure. *Physics Letters A*, 283(1-2):85–88, 2001.

[11] S Karki. S. karki et al., rev. sci. instrum. 87, 114503 (2016). *Rev. Sci. Instrum.*, 87:114503, 2016.

[12] H P Daveloza, M Afrin Badhan, M Diaz, K Kawabe, P N Konverski, M Landry, and R L Savage. Controlling calibration errors in gravitational-wave detectors by precise location of calibration forces. *Journal of Physics: Conference Series*, 363(1):012007, 2012. URL `http://stacks.iop.org/1742-6596/363/i=1/a=012007`.